Supplementary Figure S1: α Diversity for WGS Metagenome and RNA Metatranscriptome data. Shannon Index of (**A**) WGS Metagenome and (**B**) RNA Metatranscriptome data.

SFigure 1

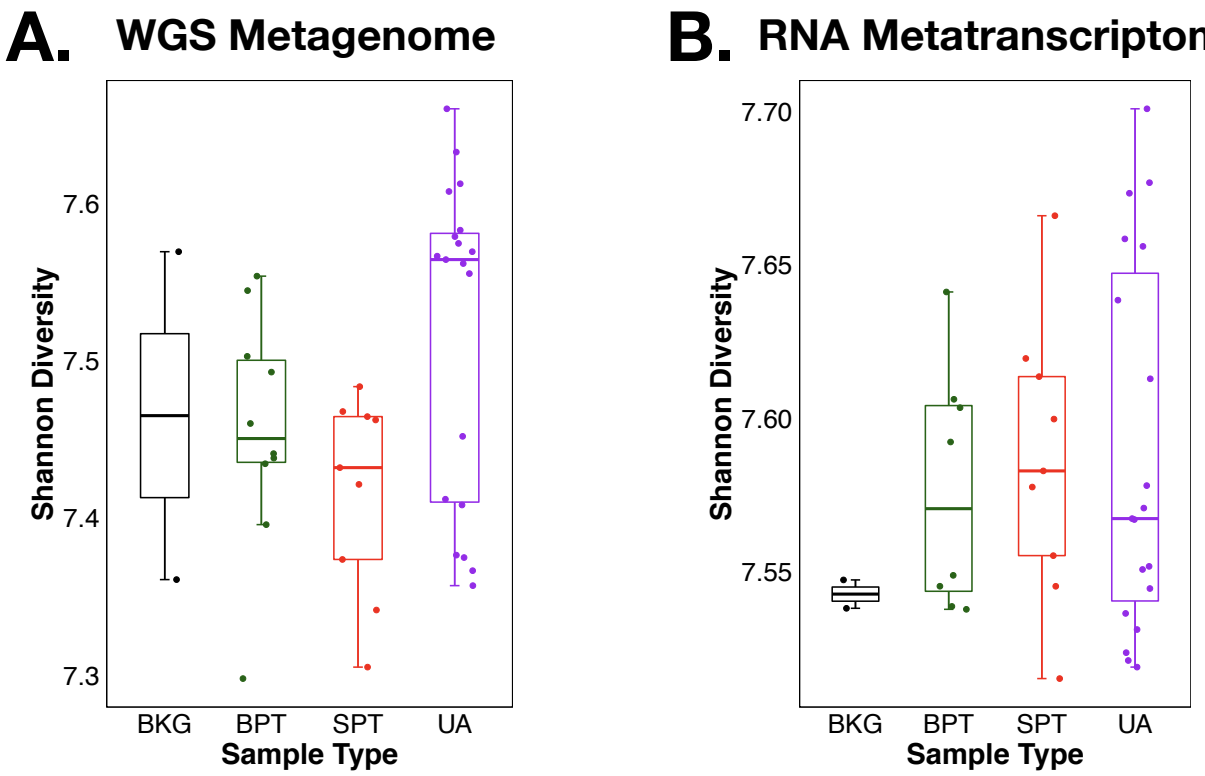
A.
WGS Metagenome
Shannon Diversity
7.6
7.5
7.4
7.3
BKG
BPT
SPT
UA
Sample Type
B.
RNA Metatranscriptome
Shannon Diversity
7.70
7.65
7.60
7.55
BKG
BPT
SPT
UA
Sample Type

Supplementary Figure S2: Rarefaction analysis for each sequencing datasets. Each line represents a sample and the dash line represents the mean for all samples. Sequence depth (x axis) is compared with OTU or KO annotation (y axis). (A) 16S rRNA gene sequencing (B) Whole Genome Sequencing (C) RNA Metatranscriptome.

SFigure 2

Rarefaction Analysis

A. 16S

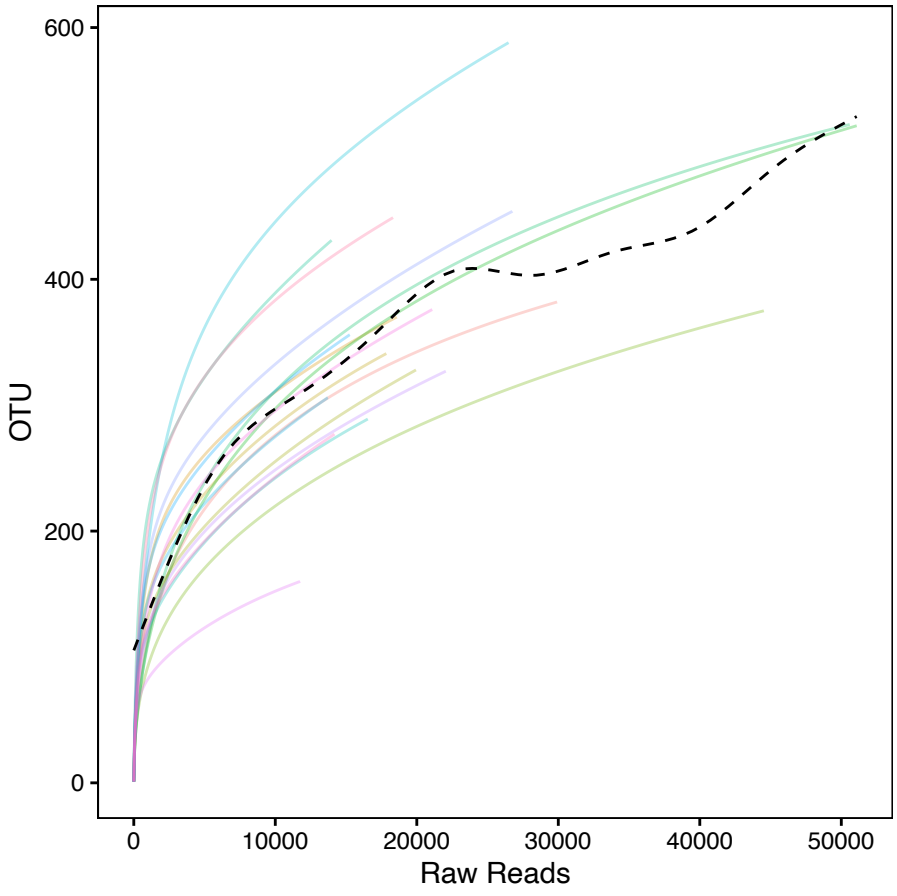

B. WGS

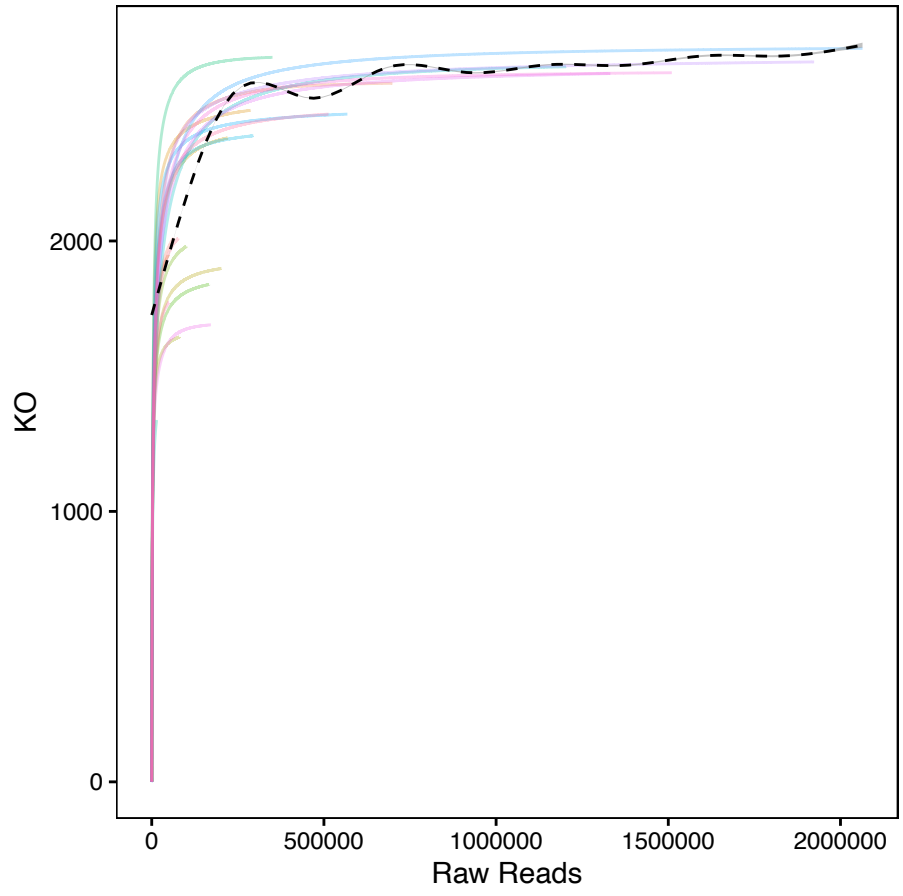

C. RNA

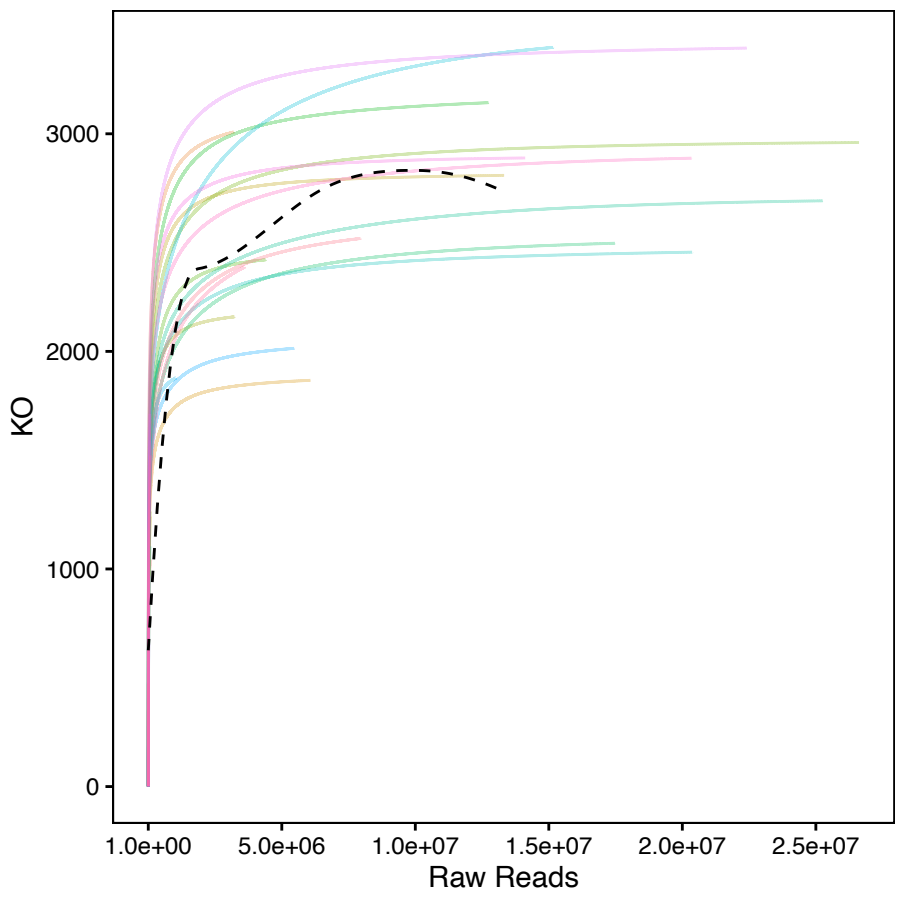

Supplementary Figure S3: Comparison of global taxonomic composition across different sequencing data types. PROCRUSTES analysis, using Bray-Curtis Distance matrices, was used to compare taxonomic annotation for the three data types. Monte-Carlo simulation test was used for statistical significance. (**A**) Comparison between 16S rRNA gene sequencing and WGS Metagenome (Monte-Carlo p-value=ns). (**B**) Comparison between 16S rRNA gene sequencing and RNA Metatranscriptome (Monte-Carlo p-value=ns). (**C**) Comparison between WGS Metagenome and RNA Metatranscriptome (Monte-Carlo p-value <0.01).

SFigure 3

Taxonomic Annotation

A. 16S vs. WGS

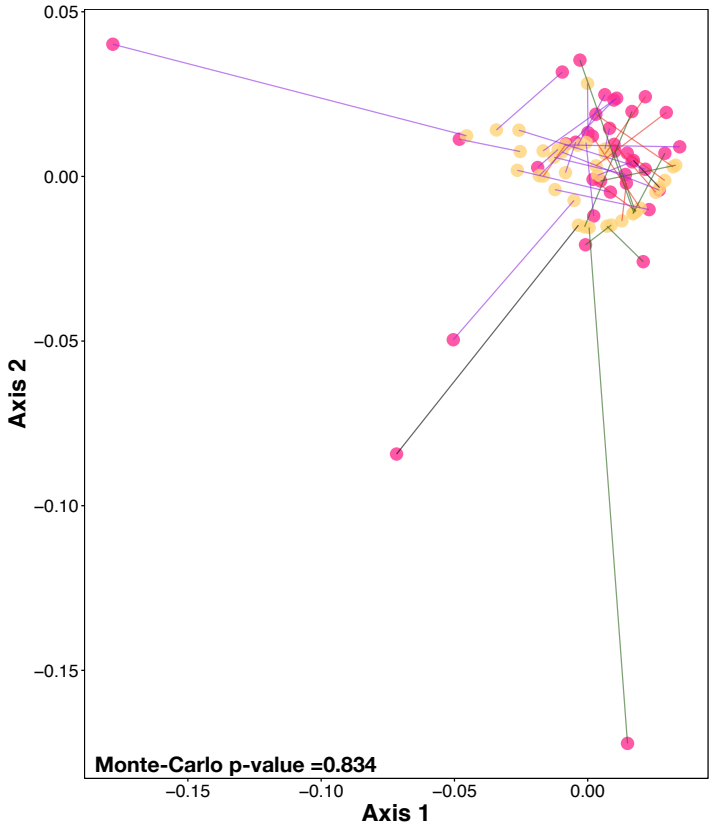

B. 16S vs. RNA

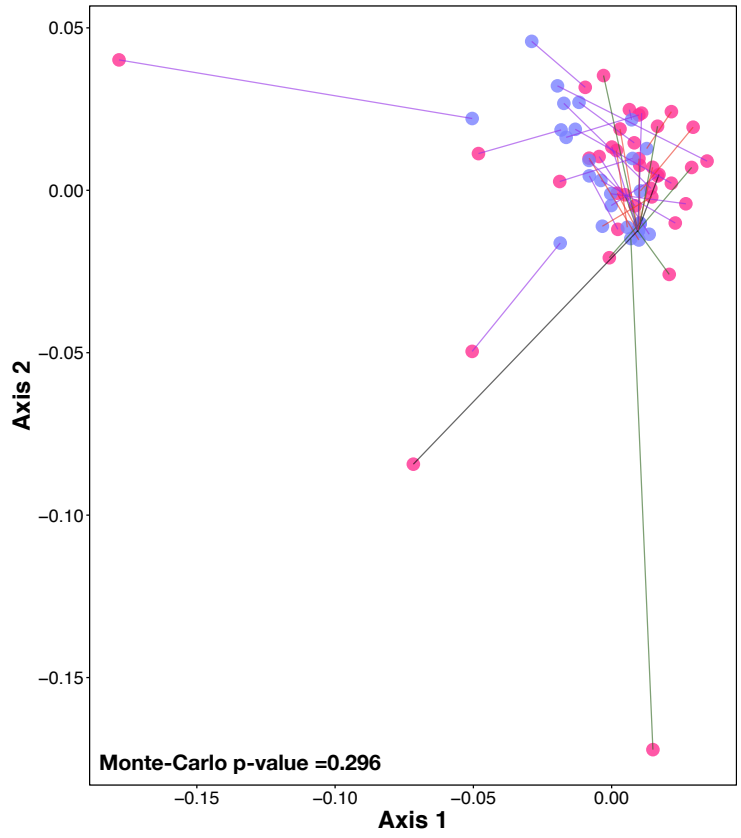

C. WGS vs. RNA

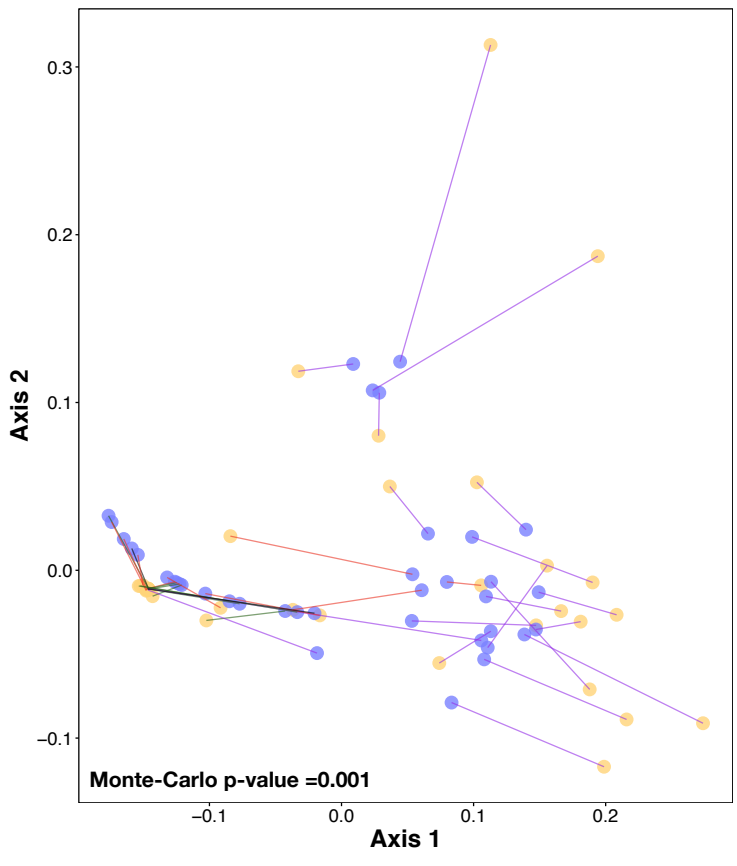

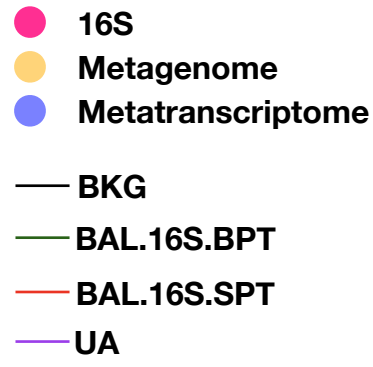

Supplementary Figure S4: Comparison of global functional composition across different sequencing data types. PROCRUSTES analysis, with Bray-Curtis Distance matrices, was used to compare functional annotation across the sequencing data types. Monte-Carlo simulation test was used for statistical significance. (**A**) Comparison between 16S rRNA gene sequencing and WGS Metagenome (Monte-Carlo p-value<0.01). (**B**) Comparison between 16S rRNA gene sequencing and RNA Metatranscriptome (Monte-Carlo p-value<0.01). (**C**) Comparison between WGS Metagenome and RNA Metatranscriptome (Monte-Carlo p-value <0.01).

SFigure 4

Functional Annotation

A. 16S vs. WGS

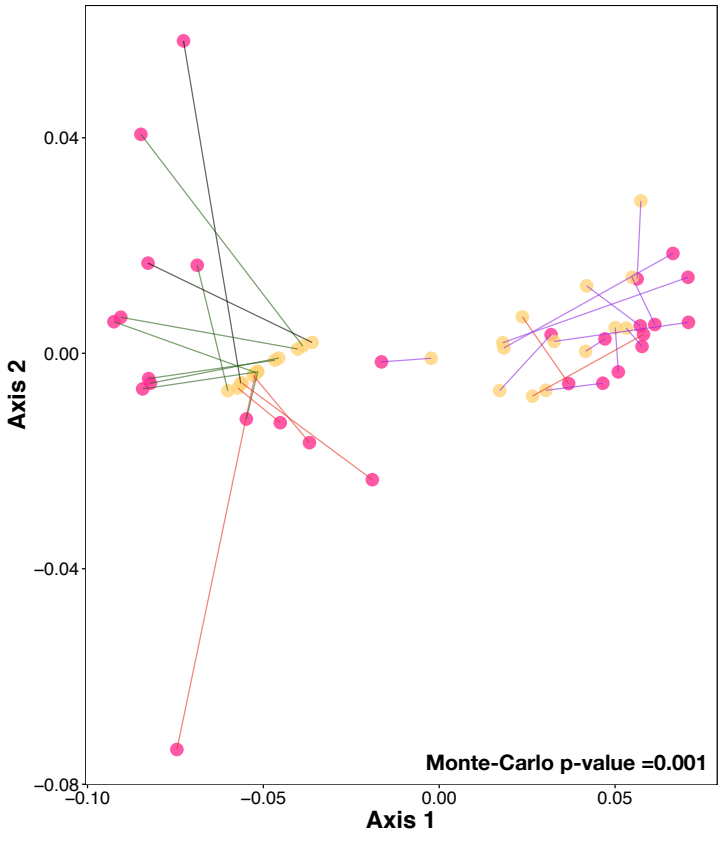

B. 16S vs. RNA

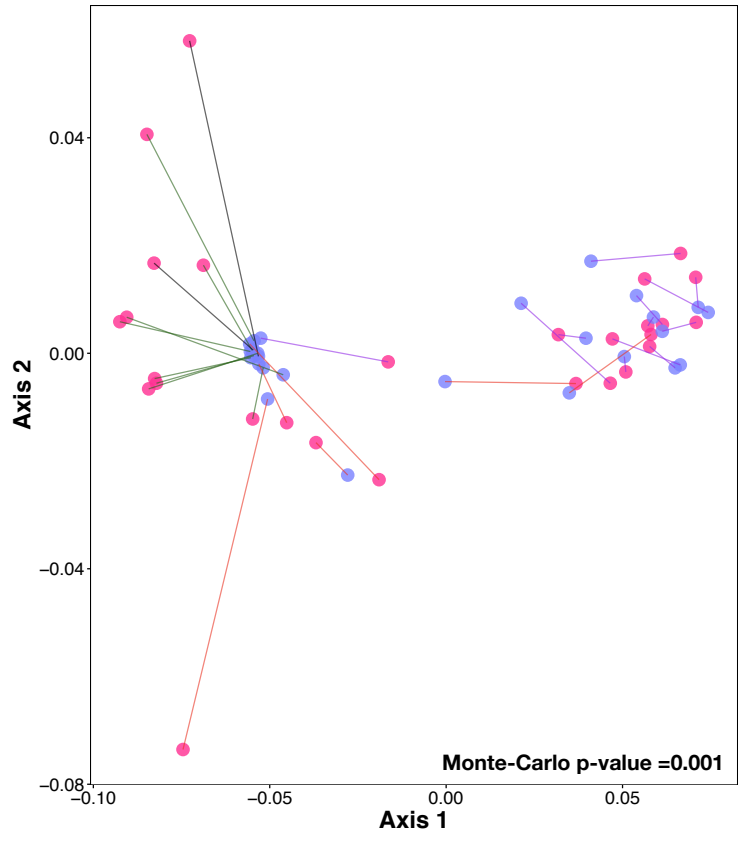

C. WGS vs. RNA

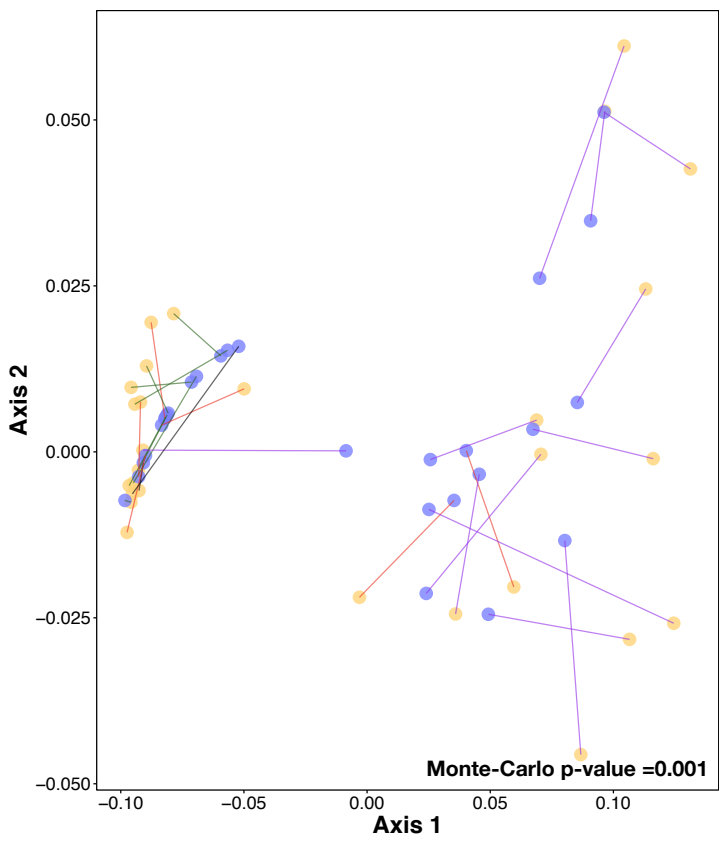

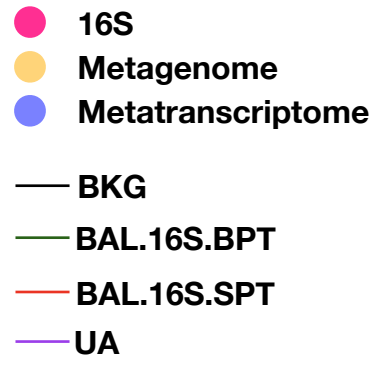

Supplementary Figure S5: Functional signatures identified as differentially enriched in BAL.SPT on WGS Metagenome and RNA Metatranscriptome data. DESEQ2 analysis of WGS Metagenome (**A**) and RNA Metatranscriptome (**B**) functional annotation identified KOs differentially enriched in BAL.16S.SPT vs. BAL.BPT.16S samples (FDR<0.05). Circle size is representative of KEGG Expression.

SFigure 5

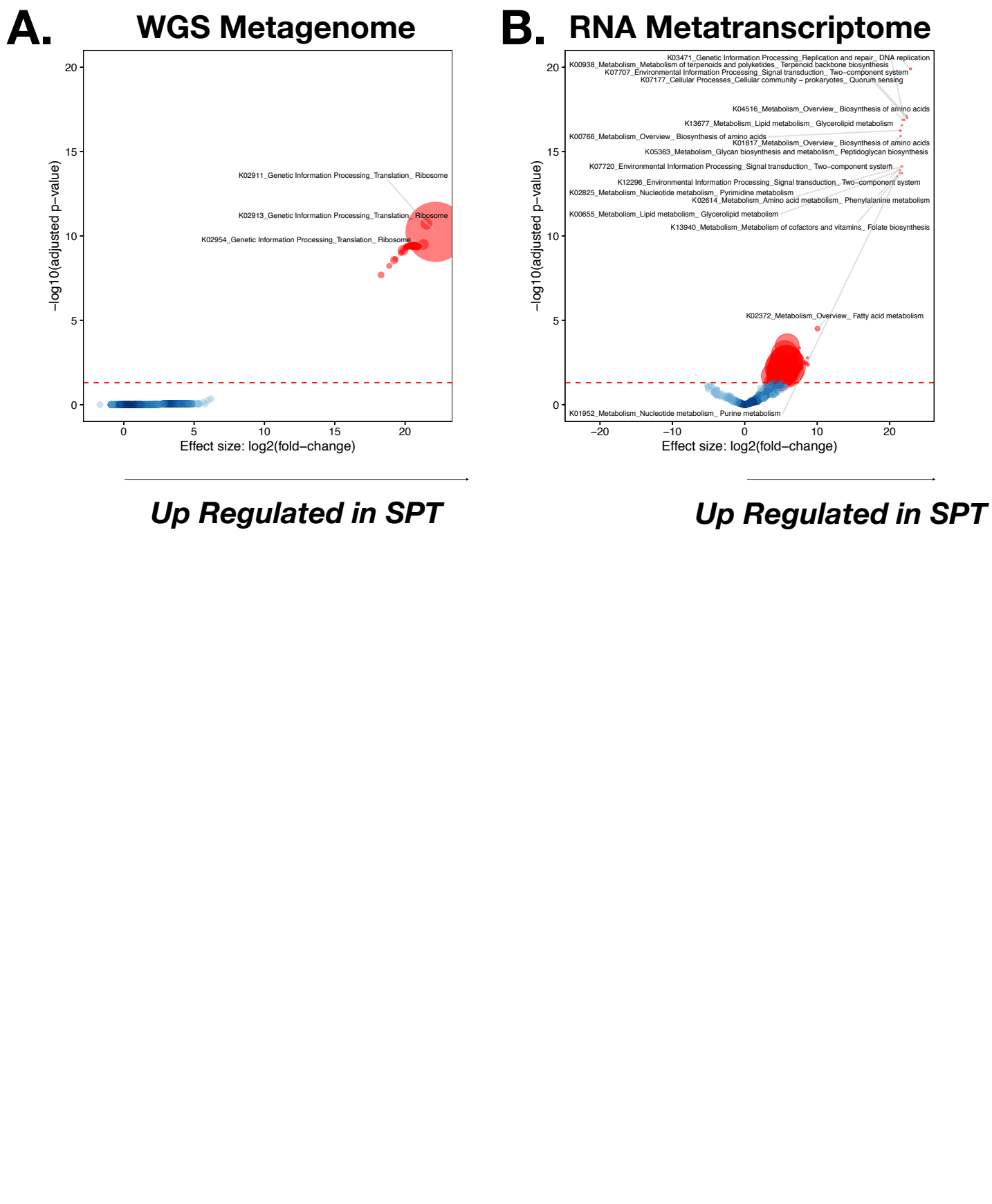
A.
WGS Metagenome
K02911_Genetic Information Processing_Translation_ Ribosome
K02913_Genetic Information Processing_Translation_ Ribosome
K02954_Genetic Information Processing_Translation_ Ribosome
−log10(adjusted p−value)
Effect size: log2(fold−change)
Up Regulated in SPT
B.
RNA Metatranscriptome
K03471_Genetic Information Processing_Replication and repair_ DNA replication
K00938_Metabolism_Metabolism of terpenoids and polyketides_ Terpenoid backbone biosynthesis
K07707_Environmental Information Processing_Signal transduction_ Two−component system
K07177_Cellular Processes_Cellular community − prokaryotes_ Quorum sensing
K04516_Metabolism_Overview_ Biosynthesis of amino acids
K13677_Metabolism_Lipid metabolism_ Glycerolipid metabolism
K00766_Metabolism_Overview_ Biosynthesis of amino acids
K01817_Metabolism_Overview_ Biosynthesis of amino acids
K05363_Metabolism_Glycan biosynthesis and metabolism_ Peptidoglycan biosynthesis
K07720_Environmental Information Processing_Signal transduction_ Two−component system
K12296_Environmental Information Processing_Signal transduction_ Two−component system
K02825_Metabolism_Nucleotide metabolism_ Pyrimidine metabolism
K02614_Metabolism_Amino acid metabolism_ Phenylalanine metabolism
K00655_Metabolism_Lipid metabolism_ Glycerolipid metabolism
K13940_Metabolism_Metabolism of cofactors and vitamins_ Folate biosynthesis
K02372_Metabolism_Overview_ Fatty acid metabolism
K01952_Metabolism_Nucleotide metabolism_ Purine metabolism
−log10(adjusted p−value)
Effect size: log2(fold−change)
Up Regulated in SPT

Supplementary Figure S6: Ex-Vivo measurement of Short Chain Fatty Acids (SCFAs) levels. (A) Levels of SCFAs in supernatant of *Veillonella parvula* in culture media were compared with media alone. Longitudinal change in levels of Butyrate (**B**) or Propionate (**C**) after ex vivo addition to BAL cells.

SFigure 6

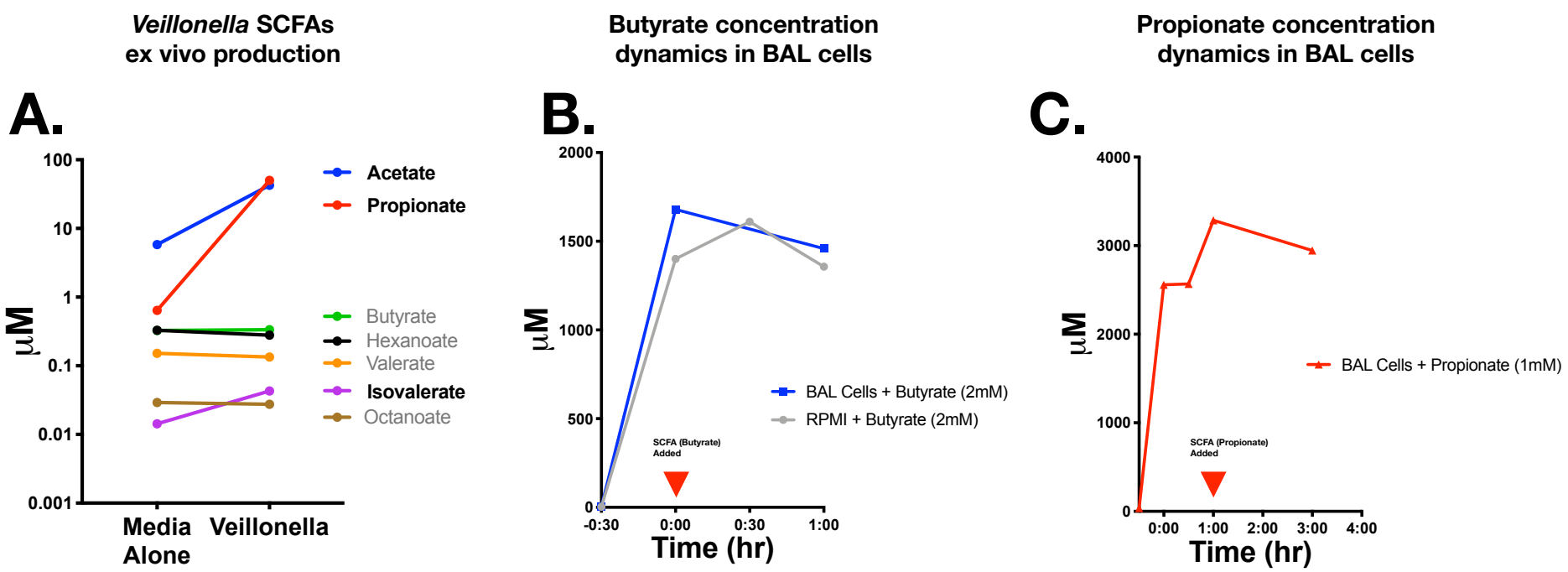
Veillonella SCFAs
ex vivo production
A.
100
10
1
0.1
0.01
0.001
µM
Media Alone
Veillonella
Acetate
Propionate
Butyrate
Hexanoate
Valerate
Isovalerate
Octanoate
Butyrate concentration
dynamics in BAL cells
B.
2000
1500
1000
500
0
µM
-0:30
0:00
0:30
1:00
Time (hr)
SCFA (Butyrate)
Added
BAL Cells + Butyrate (2mM)
RPMI + Butyrate (2mM)
Propionate concentration
dynamics in BAL cells
C.
4000
3000
2000
1000
0
µM
0:00
1:00
2:00
3:00
4:00
Time (hr)
SCFA (Propionate)
Added
BAL Cells + Propionate (1mM)

Supplementary Figure S7: Comparison of levels of SCFAs in UA and BAL samples. Correlation analysis using spearman rho showed no significant association between levels of SCFAs detected in UA and BAL samples.

SFigure 7

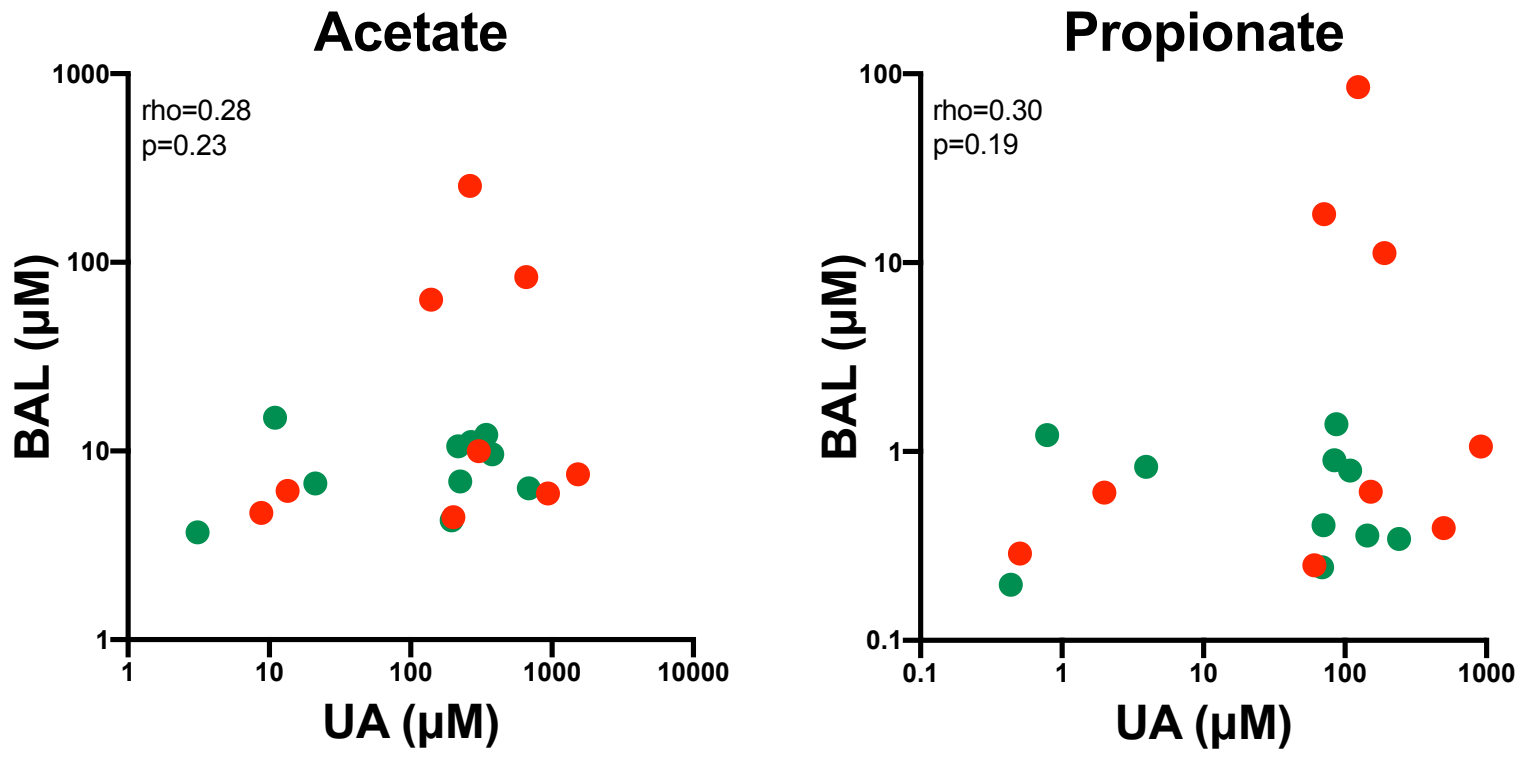
Acetate
rho=0.28
p=0.23
BAL (µM)
1000
100
10
1
1
10
100
1000
10000
UA (µM)
Propionate
rho=0.30
p=0.19
BAL (µM)
100
10
1
0.1
0.1
1
10
100
1000
UA (µM)
Isovalerate
rho=-0.04
p=0.85
BAL (µM)
1
0.1
0.01
0.01
0.1
1
10
100
UA (µM)
Butyrate
rho=0.10
p=0.66
BAL (µM)
10
1
0.1
0.01
0.1
1
10
100
UA (µM)
BAL16S.SPT
BAL16S.BPT

Supplementary Figure S8: Clustering of WGS Metagenome and RNA Metatranscriptome: Dirichlet Multinomial Modelling (DMM) of all samples was performed separately for WGS Metagenome (**A**) and RNA Metatranscriptome (**C**). In both cases, 2 clusters were identified as the best model fit. Principle Co-ordinate analysis of WGS metagenome (**B**), based on Bray-Curtis Distance, using DMM clustering of BAL samples showed that only three BAL Samples clustered with UA samples. Principle Co-ordinate analysis of RNA metatranscriptome (**C**), based on Bray-Curtis Distance, using DMM clustering of BAL samples showed that only two BAL Samples clustered with UA samples.

SFigure 8

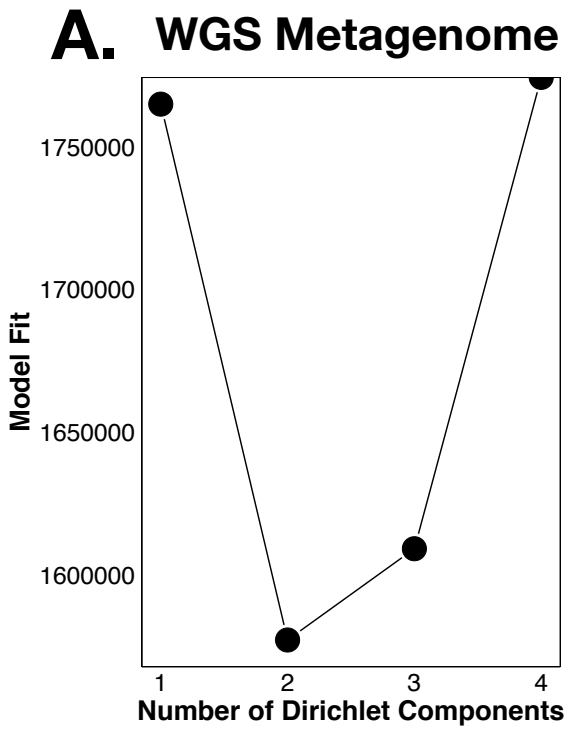
A.
WGS Metagenome
1750000
1700000
1650000
1600000
Model Fit
1
2
3
4
Number of Dirichlet Components

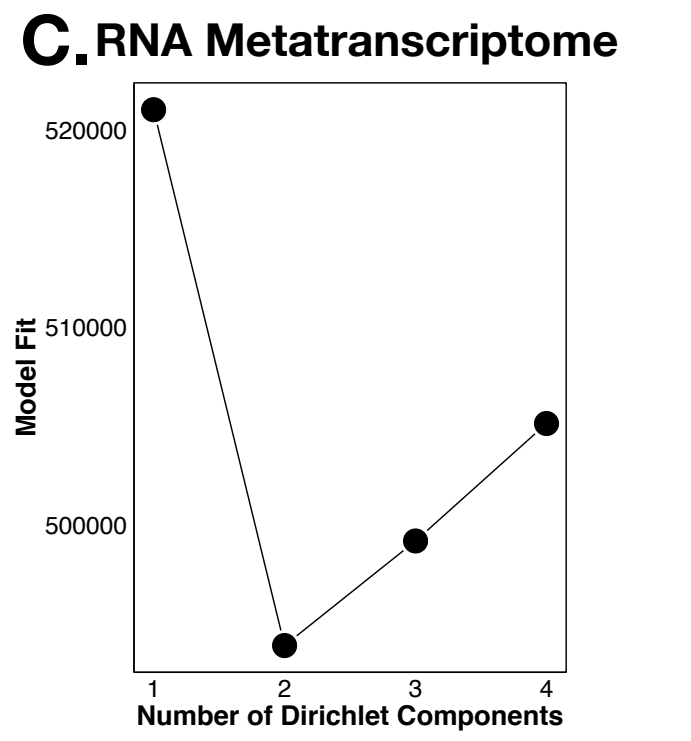
C.
RNA Metatranscriptome
520000
510000
500000
Model Fit
1
2
3
4
Number of Dirichlet Components

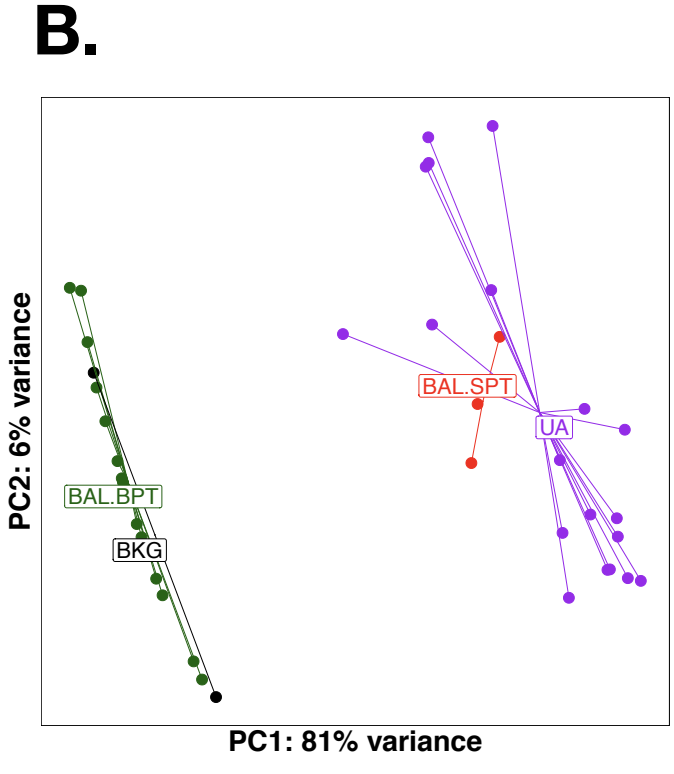
B.
PC2: 6% variance
BAL.BPT
BKG
BAL.SPT
UA
PC1: 81% variance

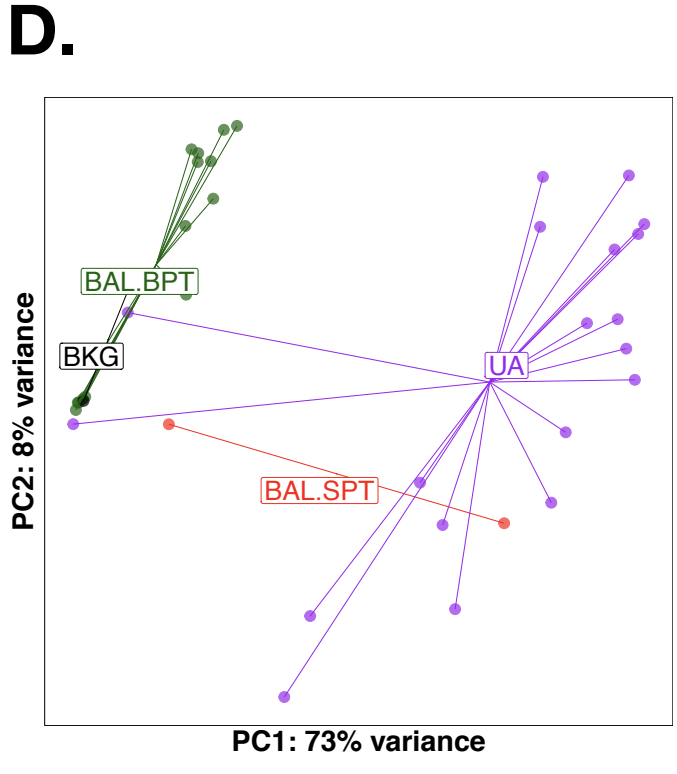
D.
PC2: 8% variance
BAL.BPT
BKG
UA
BAL.SPT
PC1: 73% variance

Supplementary Figure S9: Identifying Potential Contaminants. Using *decontam* with a threshold of 0.7, contaminants were identified based on their prevalence in BAL and Upper Airway (UA) samples when compared to Background (BKG) samples. The top taxa, identified as contaminants, median relative abundance, is displayed for the (A) 16S rRNA gene sequencing (**B**) Whole Genome Sequencing and (**C**) RNA Metatranscriptome.

SFigure 9

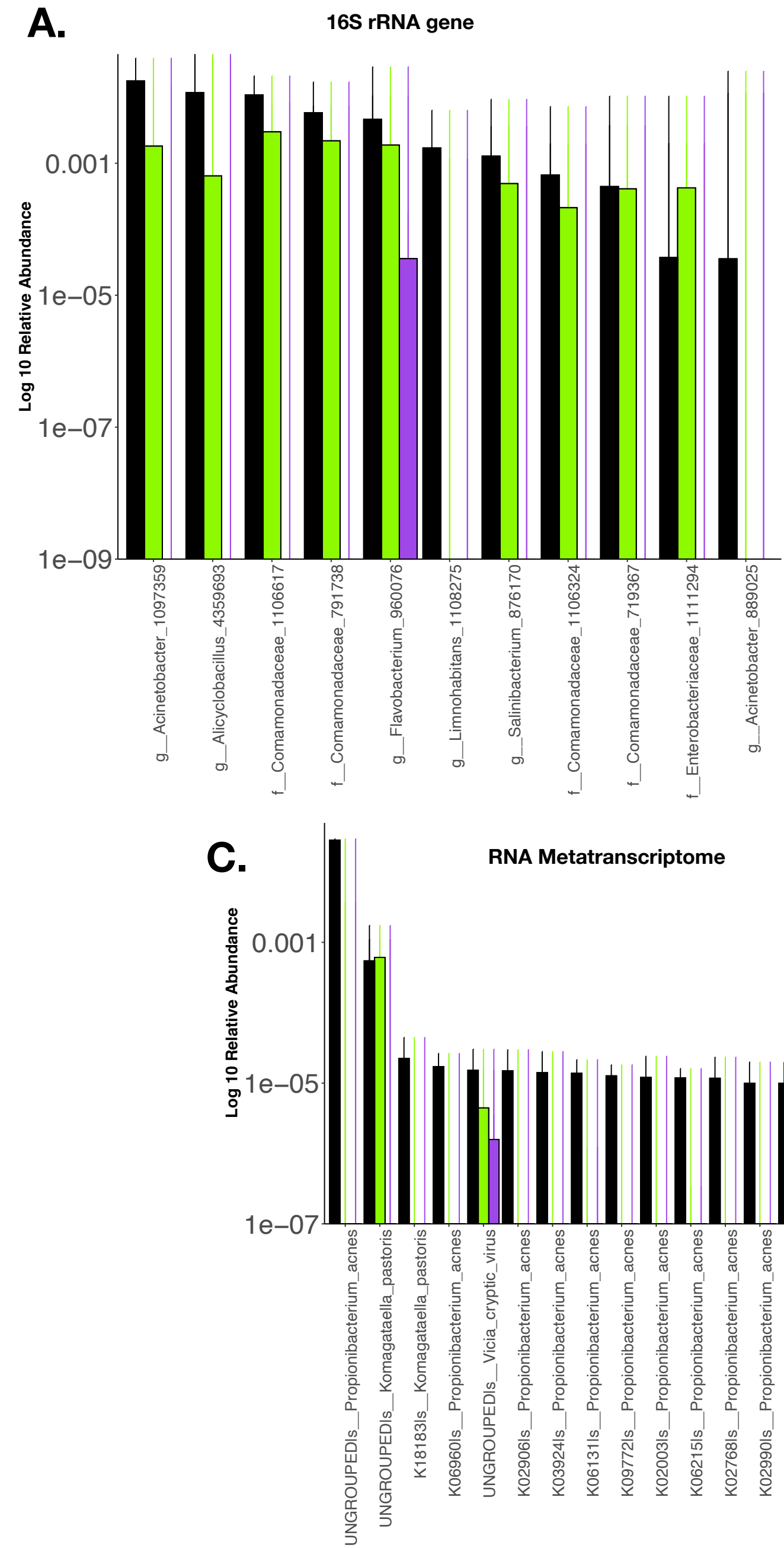
A.
16S rRNA gene
Log 10 Relative Abundance
0.001
1e−05
1e−07
1e−09
g__Acinetobacter_1097359
g__Alicyclobacillus_4359693
f__Comamonadaceae_1106617
f__Comamonadaceae_791738
g__Flavobacterium_960076
g__Limnohabitans_1108275
g__Salinibacterium_876170
f__Comamonadaceae_1106324
f__Comamonadaceae_719367
f__Enterobacteriaceae_1111294
g__Acinetobacter_889025
B.
WGS Metagenome
Log 10 Relative Abundance
0.1
0.001
1e−05
1e−07
UNMAPPED
UNGROUPED
UNGROUPEDlunclassified
C.
RNA Metatranscriptome
BKG
UA
BAL
Log 10 Relative Abundance
0.001
1e−05
1e−07
UNGROUPEDls__Propionibacterium_acnes
UNGROUPEDls__Komagataella_pastoris
K18183ls__Komagataella_pastoris
K06960ls__Propionibacterium_acnes
UNGROUPEDls__Vicia_cryptic_virus
K02906ls__Propionibacterium_acnes
K03924ls__Propionibacterium_acnes
K06131ls__Propionibacterium_acnes
K09772ls__Propionibacterium_acnes
K02003ls__Propionibacterium_acnes
K06215ls__Propionibacterium_acnes
K02768ls__Propionibacterium_acnes
K02990ls__Propionibacterium_acnes
K07742ls__Propionibacterium_acnes
K03110ls__Propionibacterium_acnes
K00338ls__Propionibacterium_acnes
K10258ls__Komagataella_pastoris
K02519ls__Propionibacterium_acnes
K04047ls__Propionibacterium_acnes